Respiratory Medicine (2014) 108, 1377–1386

Available online at www.sciencedirect.com

ScienceDirect

journal homepage: www.elsevier.com/locate/rmed

Usual interstitial pneumonia and smoking-related interstitial fibrosis display epithelial to mesenchymal transition in fibroblastic foci

Alexandre Todorovic Fabro [a,*], Igor Otavio Minatel [a], Maristela Peres Rangel [c], Iris Halbwedl [b], Edwin Roger Parra [c], Vera Luiza Capelozzi [c], Helmut Popper [b]

[a] Department of Pathology, Botucatu Medical School, São Paulo State University, Botucatu, Brazil
[b] Institute of Pathology, Medical University of Graz, Graz, Austria
[c] Department of Pathology, Faculdade de Medicina, Universidade de São Paulo, São Paulo, Brazil

Received 30 January 2014; accepted 25 June 2014
Available online 17 July 2014

KEYWORDS
Epithelial-mesenchymal transition;
Usual interstitial pneumonia;
Idiopathic pulmonary fibrosis;
Smoking-related interstitial fibrosis;
Double-staining immunohisto-chemistry

Summary
Background: Fibroblastic foci (FF) are a major histological feature of usual interstitial pneumonia (UIP) in idiopathic pulmonary fibrosis (IPF) and collagen vascular diseases (non-IPF). In addition, FF are occasionally associated with smoking-related interstitial fibrosis (SRIF). Recent studies have suggested a role for epithelial to mesenchymal transition (EMT) in pulmonary fibrogenesis.
Methods: Here, we investigated whether EMT was present in patients with IPF ($n = 19$), non-IPF ($n = 17$), and SRIF ($n = 16$) using morphometric immunohistochemistry, electron microscopy, and confocal microscopy. All patients had received lung biopsies or lobectomies for lung cancer.
Results: IPF and non-IPF patients displayed restrictive lung function patterns, whereas those with SRIF presented mixed patterns. Cells within FF presented high number of alpha-smooth muscle actin (αSMA)-staining cells; however, the foci of IPF patients showed comparatively lower number. Moreover, colocalization of thyroid transcription factor-1 (TTF1) and αSMA within FF showed low number of staining cells for IPF and SRIF in comparison to non-IPF ($p < 0.01$). Nevertheless, all groups displayed colocalization of high rate of $TTF1^{+}$-cells and

* Corresponding author. Pathology Department, São Paulo State University, HCFMB/UNESP; Campus de Rubião Junior s/n Botucatu, São Paulo 18618-970, Brazil. Tel.: +55 14 99619 5522; fax: +55 14 3815 2348.
E-mail addresses: alexandretodofabro@gmail.com, alexandretodofabro@hotmail.com (A.T.Fabro).

http://dx.doi.org/10.1016/j.rmed.2014.06.008

low rate of αSMA$^+$-cells within hyperplastic epithelioid cells in FF. Also, we observed areas with low proportion of TTF1$^+$cells and αSMA$^+$cells, which were present in SRIF and non-IPF more often than IPF ($p < 0.001$). Electron microscopy revealed small breaks in the alveolar basal lamina, which allowed epithelioid cells to directly contact the collagenous matrix and fibroblasts. Three-dimensional reconstruction revealed intense αSMA staining within some epithelioid cells, suggesting that they had gained a mesenchymal phenotype.
Conclusions: These findings constitute the first report of EMT in SRIF and suggest that EMT occurs more prominently in SRIF and non-IPF than IPF.

Introduction

Fibroblastic foci (FF) of pulmonary fibrosis are small focal areas of young, myxoid-appearing matrix that contain aggregates of collagen-producing myofibroblasts undergoing active proliferation [1—3]. These foci are often identified at the transition zone between normal uninvolved lung tissue and abnormal fibrotic regions. FF have been hypothesized to represent local remodeling events during acute lung injury [2,4,5] and are believed to recapitulate processes occurring during the healing of skin wounds [6]. In particular, FF are clinically and biologically important in disease progression, with the amount of FF observed in surgical lung biopsies directly correlating with progressive physiologic deterioration and shortened survival in patients with IPF [7,8]. However, the role of FF in SRIF and non-IPF patients is not established.

FF are a major histological feature of usual interstitial pneumonia (UIP). Examples of causes of UIP include systemic sclerosis/scleroderma (non-IPF), idiopathic pulmonary fibrosis (IPF), rheumatoid arthritis, asbestosis and chronic nitrofurantoin toxicity [9,10]. In addition, FF are occasionally found in patients with smoking-related interstitial fibrosis (SRIF) [11] and may play a critical role in the development of this fibrosing lung disease. Although FF are clinically relevant, the mechanisms involved in their cellular origin and formation remain ill defined.

Recent *in vitro* and animal studies have suggested that epithelial to mesenchymal transition (EMT) of alveolar epithelial cells occurs during pulmonary fibrogenesis. EMT is the process by which epithelial cells lose their phenotypic characteristics and acquire features of mesenchymal cells, such as fibroblasts and myofibroblasts. Indeed, pulmonary fibrosis-associated EMT has been observed with experimental models [12,13], as well as *in vitro* [14,15] and human studies [16—18]. Moreover, EMT has been identified during embryonic differentiation [19], tumor progression [20], renal fibrosis [21], and liver fibrosis [22]. Therefore, we hypothesized that EMT might represent a general phenomenon occurring during pulmonary fibrogenesis, which is not only IPF specific. Here, we employed immunohistochemistry, electron microscopy, and confocal microscopy to investigate whether EMT was present in tissue sections from IPF, non-IPF, and SRIF patients.

Materials and methods

Characteristics of human subjects and inclusion criteria

Between 2006 and 2011, we consecutively enrolled patients with IPF ($n = 19$), non-IPF ($n = 17$), and SRIF ($n = 16$) who underwent open or thoracoscopic lung biopsy or lobectomy for lung cancer in our hospitals. Three lung pathologists (ATF, VLC, and HP), who were unaware of the clinical and physiologic findings, independently reviewed the lung biopsies. In cases where the classification by these pathologists differed, a consensus opinion on the overall histopathologic pattern was reached. Histologic features of UIP were based on a previously published report [23] and the criteria of the American Thoracic Society/European Respiratory Society (ATS/ERS) classification [9]. SRIF represented a secondary diagnosis in smoking patients with co-existing neoplastic disease, and its histologic features were based on a previously published report by Katzeinstein and colleagues [11]. Both non-IPF and IPF patients presented with the characteristic histopathologic pattern associated with UIP. The study protocol was approved by the Ethical Committee of Graz University, Austria (Number 24—135 ex 11/12). Notably, patients in an accelerated phase of interstitial pneumonia were excluded. Also, all non-IPF patients fulfilled the histological and clinical criteria for systemic sclerosis.

Immunohistochemistry

To simultaneously characterize epithelial and mesenchymal markers we employed a double-staining immunohistochemistry protocol, which utilized antibodies against thyroid transcription factor-1 (TTF1; mouse monoclonal, DAKO, Clone 8G7G3/1) and alpha-smooth muscle actin (αSMA; mouse monoclonal, DAKO Clone 1A4). Briefly, sections were deparaffinized, fixed in acetone (5 min, 22 C), and rehydrated in phosphate-buffered saline (PBS; pH 7.4) for 10 min. Immunohistochemistry was performed using a horseradish peroxidase labeled streptavidin biotin kit (HRP-LSAB, DAKO), as recommended by the manufacturer. After incubation with blocking solution (5 min), the sections were incubated for 30 min with one primary antibody (diluent from DAKO), followed by sequential 15 min incubations with biotinylated antibody (goat anti-mouse) and

peroxidase-labeled streptavidin. The slides rinsed twice with distilled water to not mix the different antibodies. The same process was performed with the second primary antibody (sequential staining). Visualization was achieved through HRP-based reactions (TTF1, brown; αSMA, red), which were terminated by washing with distilled water. The sections were then counterstained with Mayer's hemalum and mounted with Kaiser's glycerol gelatin (Merck, Vienna, Austria).

Histological disease status in IPF, non-IPF, and SRIF was assigned based on the expression of markers in regions containing hyperplastic cells within and overlying FF. Indeed, the number of established foci present in IPF lung tissue relates to disease severity and the rate of disease progression [8]. A modified quantitative assessment was performed for each individual biopsy as previously reported by Nicholson and colleagues [8].

Quantification of FF

Lung specimens were obtained from at least two lobes, and all available specimens were reviewed. Hematoxylin/eosin-stained sections were viewed at a 100-fold magnification, and the number of FF were counted. In addition, digital images captured at 400-fold magnification were used to examine the expression of epithelial and mesenchymal markers in cells within and overlying FF in IPF, non-IPF, and SRIF sections. All hyperplasic and fusiform cells were counted, and the number of cells expressing each marker was counted. In order to assess the intraobserver variability for this quantitative method, the same pathologist reviewed each specimen in different days. Additionally, interobserver variability was examined by requiring two pathologists (HP and ERP) to independently review each specimen.

Transmission electron microscopy (TEM)

To avoid the small nests of tangentially-sectioned, entrapped alveolar epithelium that could be observed in immunohistochemistry, we also performed electron microscopy. Following fixation with 3% glutaraldehyde in 0.1 M cacodylate buffer (pH 7.3) and a 1 h treatment with 1% osmium tetroxide (in the same buffer), tissues were processed using standard TEM methods. Thin sectioning was performed to trim FF-containing areas for the non-IPF samples.

Three-dimensional reconstruction analysis

Colocalization of mesenchymal (αSMA) and epithelial (TTF1) markers was assessed via immunofluorescence and confocal microscopy. Briefly, lung biopsies were incubated with antibodies against TTF1 and αSMA (same monoclonal antibodies used for immunohistochemistry) followed by double staining with fluorescein- and rhodamine-conjugated goat anti-mouse IgG (dilution 1:40, Santa Cruz Biotechnology, Santa Cruz, CA). All images were obtained using a Zeiss LSM-410 laser-scanning confocal microscope. Serial optical sections were performed with Simple 32 C-imaging computer software (LSM Image Browser software, Carl Zeiss). Z-series sections were collected every 0.6 μm with an X60 Plan Apo lens and a scan zoom of X2. The images were collected using identical photomultiplier tube settings, and they were processed and reconstructed with NIH Image software.

Data collection

We collected data on patient characteristics (i.e., sex, age, and smoking history) and assessed pulmonary function at the time of surgical lung biopsy.

Statistical analysis

Data are expressed as means (standard deviation of the mean) with 95% confidence intervals. We performed statistical analyses of variance, which were followed by appropriate post-hoc tests. The Bonferroni correction was used for multiple comparisons, whereas the one-way

Table 1 Clinical data of patients with idiopathic pulmonary fibrosis, non-idiopathic pulmonary fibrosis, and smoking-related interstitial fibrosis.

	IPF/UIP	Non-IPF/UIP	SRIF	*P*-value
Number	24	30	20	
Males/females	16/8	26/4	16/4	NS
Age at biopsy (years)	65 ± 9	54.7 ± 7.91	61.2 ± 6.21	NS
Spirometry				
FEV_1 (% pred)	70.5 ± 14.42	77.58 ± 20.06	73.2 ± 9.22	NS
FVC (% pred)	65 ± 13.85	70.87 ± 16.88	64.9 ± 11.95	NS
FEV_1/FVC (% pred)	107.96 ± 8.70	92.75 ± 18.55	60.22 ± 9.39	NS
TLC (% pred)	81 ± 11.57	77.55 ± 20.32	79.27 ± 25.01	NS
RV (% pred)	117.5 ± 35.52	98.21 ± 61.14	111.13 ± 50.67	NS
*D*LCO (% pred)	66.86 ± 21.68	56.27 ± 23.18	63.72 ± 15.29	NS
*D*LCO/AV (% pred)	77.76 ± 37.28	55.66 ± 31.62	59.11 ± 40.41	NS

Data are represented as means ± standard deviations. IPF/UIP = idiopathic pulmonary fibrosis/usual interstitial pneumonia; non-IPF/UIP = non-idiopathic pulmonary fibrosis/usual interstitial pneumonia; FEV_1 = forced expiratory volume in 1 s; FVC = forced vital capacity; TLC = total lung capacity; RV = residual volume; DLCO = diffusing capacity of the lung for carbon monoxide; VA = alveolar volume.

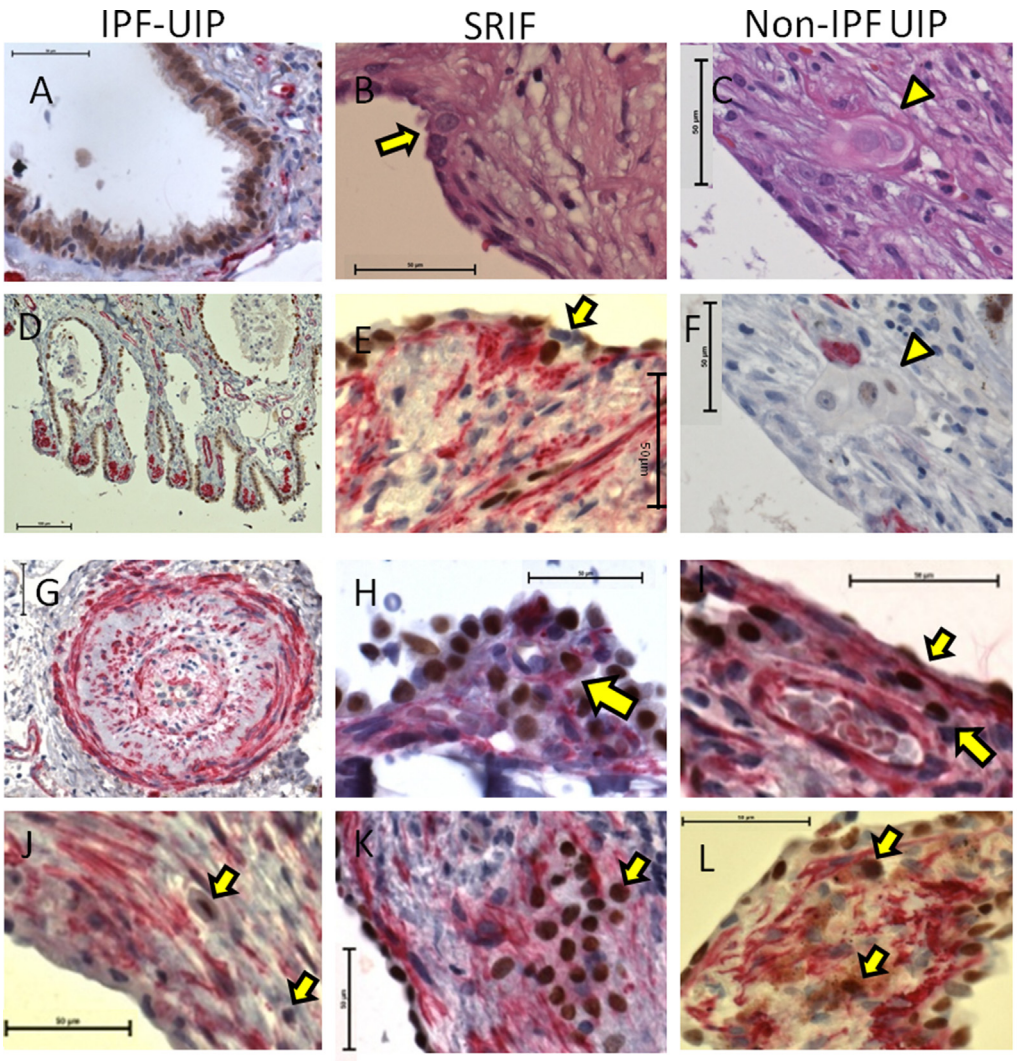
IPF-UIP
SRIF
Non-IPF UIP
A
B
C
D
E
F
G
H
I
J
K
L
50µm

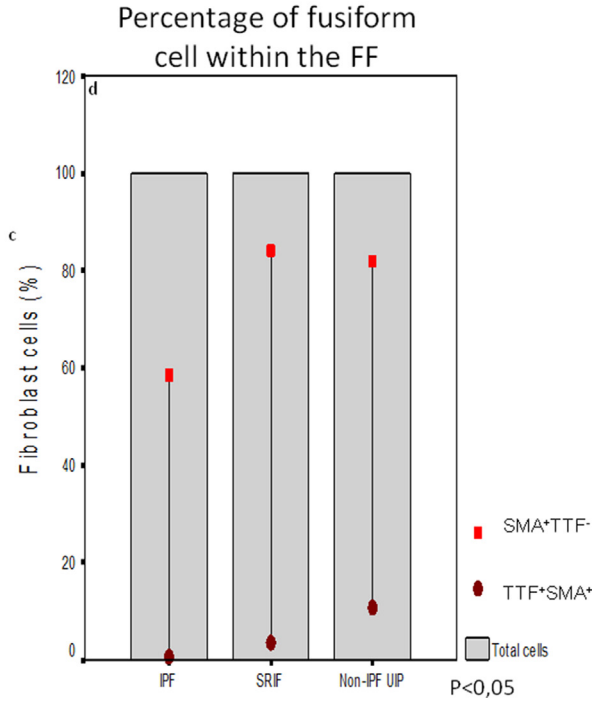
Percentage of fusiform cell within the FF
Fibroblast cells (%)
120
100
80
60
40
20
0
IPF
SRIF
Non-IPF UIP
SMA+TTF-
TTF+SMA+
Total cells
P<0,05

Table 2 Summary of quantitative results.

	IHC		Number of FF	Mean % of cells	Standard error	*P*-value
Cells within FF	$TTF1^+$ αSMA^+	IPF	122	0.65	0.50	Non-IPF × IPF <0.01
		SRIF	41	3.65	1.66	Non-IPF × SRIF = 0.01
		Non-IPF	86	10.93	2.14	
	$TTF1^-$ αSMA^+	IPF	122	58.60	2.67	SRIF × IPF <0.01
		SRIF	41	83.90	1.04	Non-IPF × IPF <0.01
		Non-IPF	86	81.86	1.74	
Cells overlying FF	$TTF1^+$ αSMA^-	IPF	115	66.52	3.06	SRIF × IPF <0.01
		SRIF	39	88.71	0.91	Non-IPF × IPF <0.01
		Non-IPF	80	85.00	1.81	
	$TTF1^-$ αSMA^+	IPF	115	1.91	0.53	SRIF × IPF = 0.003
		SRIF	39	6.41	1.39	
		UIP-L	80	3.37	0.92	
	$TTF1^-$ αSMA^-	IPF	115	41.56	2.80	IPF × SRIF <0.01
		SRIF	39	19.48	3.09	IPF × Non-IPF < 0.01
		Non-IPF	80	24.25	2.90	
	$TTF1^+$ αSMA^+	IPF	115	1.82	0.455	SRIF × IPF = 0.001
		SRIF	39	8.46	2.53	Non-IPF × IPF = 0.001
		Non-IPF	80	6.87	1.20	

Data are presented as means ± standard deviations of two lung specimens obtained by open surgical biopsy or lobectomy in each patient (all microscopic fields were analyzed in each specimen). Epithelial and mesenchymal markers were detected by immunostaining (TTF1 and αSMA, respectively). All lung specimens were analyzed for number of FF by case, percentage of $TTF1^+$ αSMA^+ cells within FF, percentage of $TTF1^-$ αSMA^+ cells within FF, percentage of $TTF1^+\alpha SMA^+$ alveolar epithelial cells overlying FF, percentage of $TTF1^+$ αSMA^- alveolar epithelial cells overlying FF, percentage of $TTF1^-\alpha SMA^-$ alveolar epithelial cells overlying FF, and percentage of $TTF1^-\alpha SMA^+$ alveolar epithelial cells overlying FF. The one-way analysis of variance (ANOVA) test and the student's *t*-test were used to compare two variables between groups. A p-value < 0.05 was considered as significant.

analysis of variance (ANOVA) test and student's *t*-test were employed when comparing two variables. All analyses were performed using SPSS 18.0 (SPSS Inc., Chicago, IL, USA). A p-value of <0.05 was considered to be significant.

Results

Clinical features

The clinical features of the patients included in this study are presented in Table 1. 24 patients with IPF, 30 patients with non-IPF, and 20 patients with SRIF were consecutively included. Patients with IPF and non-IPF displayed restrictive lung function patterns, which were characterized by decreased total lung capacity (81% and 79% of predicted values for IPF and non-IPF). Also, the FEV_1/FVC ratio/100 increased in IPF and non-IPF. However, the predicted values for DLCO and DLCO/VA in IPF and non-IPF did not significantly differ (Table 1). SRIF patients usually presented with mixed lung function patterns (restrictive and obstructive; due to emphysema and concomitant tumor).

Immunohistochemistry

In control lung samples, which were obtained from autopsy, TTF1 expression (epithelial marker) could be visualized within the nuclei of bronchiolar, alveolar, and hyperplastic epithelial cells (brown staining; Fig. 1A and D). In contrast, αSMA (mesenchymal marker) was observed in smooth muscle cells within the walls of remodeled arteries in IPF (Fig. 1G). Notably, we found differential number of TTF1- and αSMA-immunostaining cells within and overlying FF in IPF, SRIF, and non-IPF. A total of 234 FF were counted (115 in IPF, 39 in SRIF, and 80 in non-IPF).

Fusiform cells could be visualized within FF from the IPF, SRIF, and non-IPF sections (Fig. 1J; B,E,H,K; and C,F,I,L, respectively). Although these cells displayed low percentage of TTF1-staining cells (<11%), the rate of TTF1-expressing cells were found to be significantly higher in the non-IPF samples. As expected, the proportion of αSMA-staining cells was high in the FF resident cells; however, the IPF group displayed overall lower rate of αSMA expression than the others (see Table 2 for quantitative results; Fig. 1J).

Figure 1 Hematoxylin and eosin staining (B–C) and dual immunohistochemical staining for αSMA (red) and TTF1 (brown) (A, D–L) within fibroblastic foci of IPF UIP (G, J), SRIF (E, H, K), and non-IPF UIP (F, I, L). The internal control was positive for TTF1 and αSMA as demonstrated by staining of the bronchiolar epithelium (A), emphysematous alveolar septum (D), and muscular layer of the arteriole (with vascular remodeling) (G) in IPF UIP. $TTF1^+$ αSMA^+ cells can be observed within fibroblastic foci in IPF-UIP (J), SRIF (B, E, H, K), and non-IPF UIP (I, L) (arrows), indicating that a population of epithelial cells underwent epithelial to mesenchymal transition. However, epithelioid cells displaying only weak expression of TTF1 can also be seen within fibroblastic foci (arrowhead) (C, F). The graph shows the percentage of $TTF1^+$ and/or αSMA^+ cells within fibroblastic foci. (For interpretation of the references to color in this figure legend, the reader is referred to the web version of this article.)

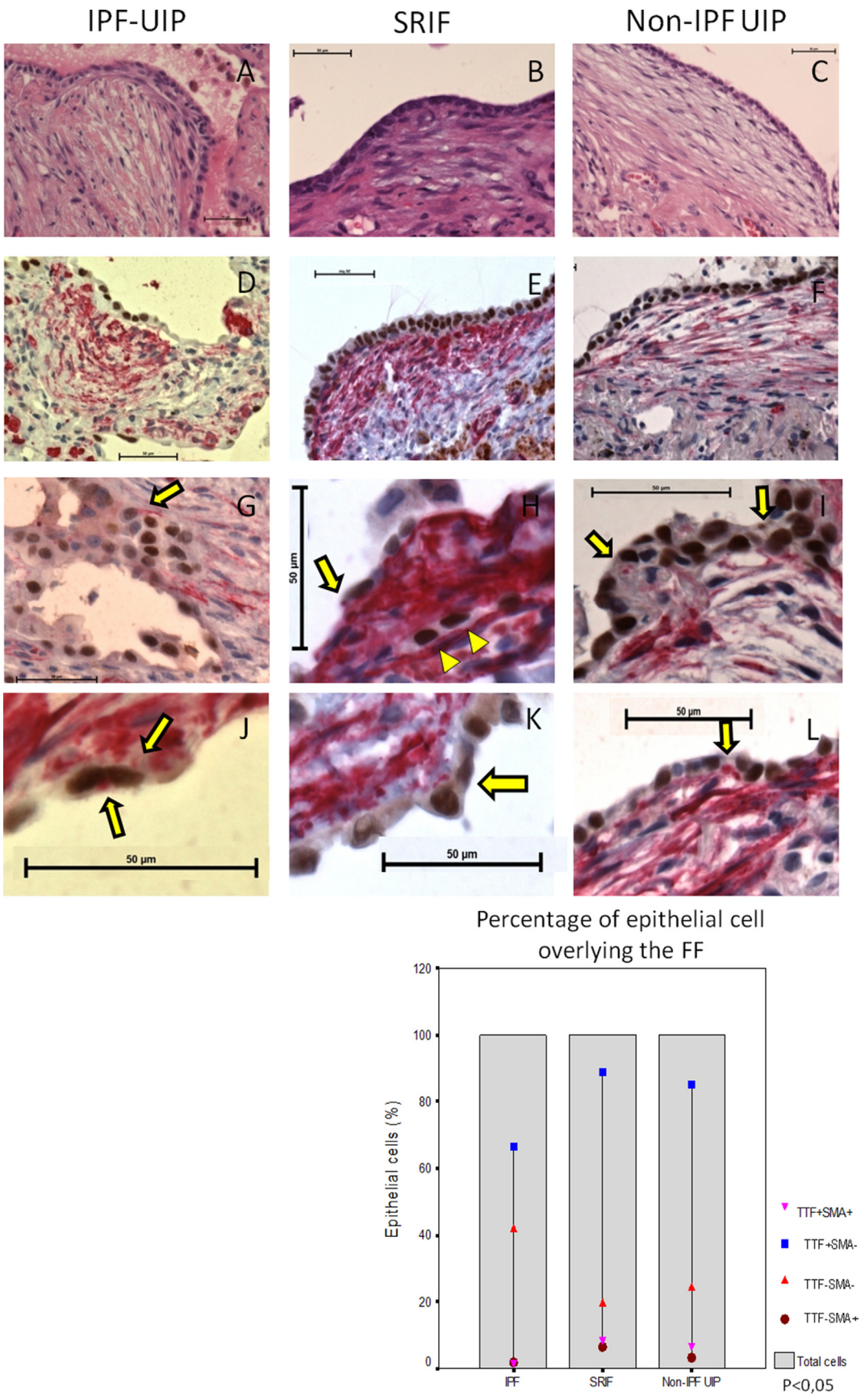

Figure 2 Hematoxylin and eosin staining (A—C) and dual immunohistochemical staining for αSMA (red) and TTF1 (brown) (D—L) overlying fibroblastic foci of IPF UIP (A, D, G, J), SRIF (B, E, H, K), and non-IPF UIP (C, F, I, L). The fibroblastic foci display

As expected, hyperplastic epithelioid cells overlying the FF in IPF (Fig. 2A, D, G and J), SRIF (Fig. 2B, E, H and K), and non-IPF (Fig. 2C, F, I and L) showed high rate of TTF1-staining cells (>65%) and low percentage of αSMA-expressing cells (<7%). However, higher rate of TTF1- and αSMA-expressing cells was observed in the SRIF group ($p < 0.01$; Table 2; Fig. 2M). Strikingly, in all of the groups, we detected co-expression of epithelial and mesenchymal markers by individual epithelioid cells that were localized in FF and near septal walls. Nevertheless, this phenomenon was more evident in cells overlying FF in SRIF compared to IPF ($p = 0.001$; Table 2; Fig. 2M).

Electron microscopy

As can be seen in Fig. 3A-E, We employed electron microscopy in order to confirm that co-expression of epithelial and mesenchymal markers was not simply an artifact of analyzing alveolar epithelium surrounded by fibroblast-rich connective tissue. Electron micrographs of FF were performed in all groups. We exemplify the findings in non-IPF case (Fig. 3). They revealed a central region containing a mixed population of type 2 alveolar epithelial cells (AEC2), amorphous extracellular matrix, fibroblasts, and neutrophils (Fig. 3A). However, the periphery of the FF was composed almost exclusively of AEC2, displaying prominent lamellar bodies (LB) (Fig. 3B). Also, densely packed structures resembling smooth muscle fibers were often present (Fig. 3C). The matrix surrounding the AEC2 contained only sparse collagen fibrils. Furthermore, strands of moderately electron dense materials were present close to the cells, which followed the plasma membranes or extended out into the matrix in an irregular fashion (Fig. 3D). Although these strands were of similar electron density to basal lamina, they lacked the uniform thickness of basal lamina. Also, high magnification revealed that they were composed of straight fibrils embedded in a finely granular material, which commonly obscured parts of the fibrils. The surface of the FF was only partially covered by AEC2, usually near sites of attachment to alveolar walls. However, no basal lamina was present beneath the epithelium, allowing the epithelium to make direct contact with the matrix of the FF. Notably, at the point where the FF contacted alveolar walls, small breaks appeared in the alveolar basal lamina, which appeared to have a sinuous or pleated contour. Basal lamina was often absent at the surface of foci, allowing AEC2 to rest directly on the collagenous matrix and at times contact fibroblasts (Fig. 3E). Even in cases where foci displayed surface basal lamina, it was often fragmented and convoluted, showing infoldings into the stroma. All groups showed the same finding, however the rate was higher in non-IPF cases.

Three-dimensional reconstruction

Immunofluorescence images obtained via confocal microscopy verified the uniform distribution of greenish nuclear TTF1 staining in control lungs in type 2 pneumocytes (Fig. 4A) and in hyperplastic type 2 alveolar epithelial cells (AEC2) (Fig. 4B). However, in IPF, non-IPF and SRIF lungs, greenish nuclear TTF1 staining of hyperplastic AEC2 showed a diffuse distribution pattern within the FF (Fig. 4C and G). Also, reddish cytoplasmic αSMA immunoreactivity was observed in hyperplastic AEC2 in IPF (Fig. 4C and D), non-IPF (Fig. 4E) and SRIF (Fig. 4F and G). In contrast, αSMA was absent from AEC2 in the control group (Fig. 4B). Using dual immunofluorescence staining (TTF1 and αSMA), we confirmed that metaplastic regenerated epithelial cells residing in the FF simultaneously expressed epithelial and mesenchymal markers (Fig. 4C–G; arrow), suggesting the occurrence of EMT (or possibly mesenchymal to epithelial transition [MET]) in all groups, however the rate of double staining cells was higher in non-IPF cases.

In summary, we have observed significant co-expression of epithelial and mesenchymal markers in FF, which is consistent with the presence of mixed-phenotype cells (i.e., myofibroblast and pneumocyte) and the occurrence of EMT in SRIF and non-IPF.

Discussion

We demonstrated *in vivo*, *in situ* and in human lung samples the presence and frequency of EMT through both epithelial and mesenchymal markers coexpression in IPF/UIP, non-IPF/UIP and, for the first time, in SRIF, suggesting that EMT is a general mechanism to pulmonary fibrosis and may contribute significantly to understanding the pathogenesis of these disorders. . Our approach was objective by use histomorphometry as a quantitative method. FF are a major histological feature of UIP in IPF, some collagen vascular diseases (non-IPF), and occasional cases of SRIF. However, the source of these myofibroblast clusters remains to be determined. Although some evidence has suggested a possible role for EMT as part of this process, it remains controversial [17,24–28]. Hosper et al. have demonstrated that collagen I is upregulated after EMT, but it is not enough to pulmonary remodeling [29]. However, these authors have studied cell culture that do not have the same microenvironment and milieu of cytokines and growth factor of human lung that promote the intense pulmonary remodeling. Furthermore, the interaction cell to cell and cell to matrix is very important to migration, fixation and transition of epithelial to mesenchymal cell.

In the current study, histological analyses revealed that epithelioid cells residing within FF in IPF were less likely to

characteristic appearances (A–C) with TTF1$^+$ epithelial cells and αSMA$^+$ myofibroblasts (D–F), which could be observed within IPF-UIP (A, D), SRIF (B, E), and Non-IPF UIP (C, F). However, some fibroblastic foci displayed rare epithelial cells, which stained with both TTF1 and αSMA in dots (arrows) (G–L), indicating that some epithelial cells underwent epithelial to mesenchymal transition. TTF1$^+$ αSMA$^+$ epithelial cells could be observed within the fibroblastic foci (arrowhead) (H). The graph shows the percentage of TTF1$^+$ and/or αSMA$^+$ epithelial cells overlying the fibroblastic foci. (For interpretation of the references to color in this figure legend, the reader is referred to the web version of this article.)

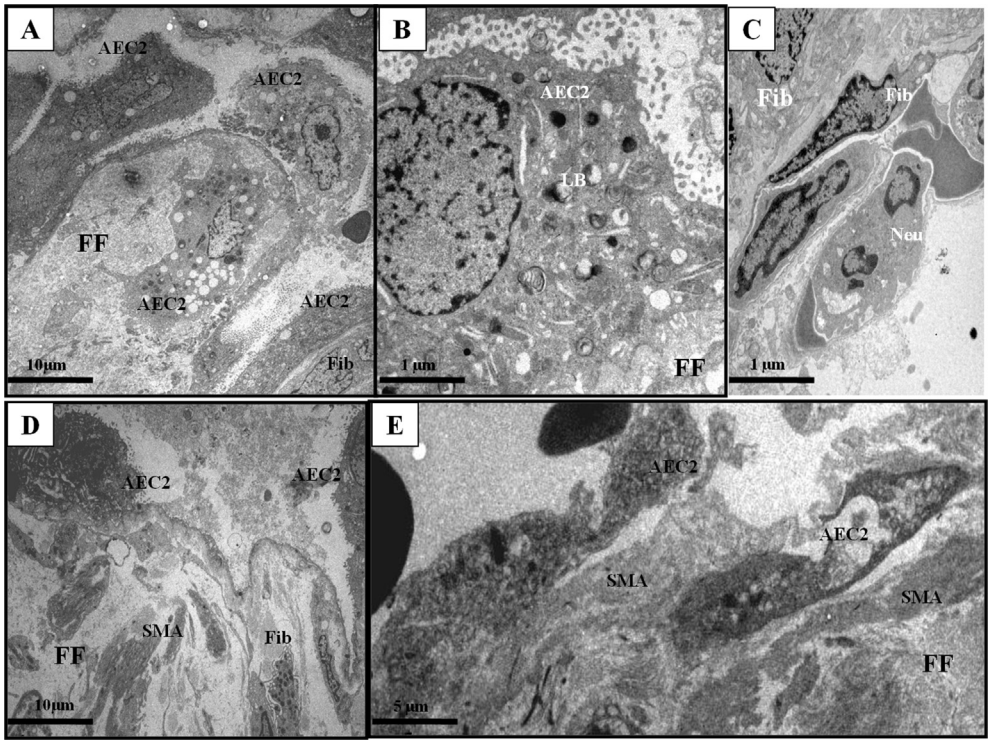

Figure 3 Electron microscopy in fibroblastic foci in non-IPF. The central region of the foci contain entrapped alveolar epithelium surrounded by fibroblast-rich connective tissue (A). The cells at the periphery of the fibroblastic foci were almost exclusively type 2 alveolar epithelial cells (AEC2) with prominent lamellar bodies (LB) (B). Note the densely compact areas resembling smooth muscle (C). The matrix surrounding these cells contained only sparse collagen fibrils in an irregular fashion (D). Small breaks in the alveolar basal lamina allowed AEC2 to rest directly on the collagenous matrix and make contact with fibroblasts (E). Fibroblast (Fib). Citrate of lead and uranile.

stain with both TTF1 and αSMA than those in SRIF and non-IPF. In addition, the number of fusiform cells within the FF that showed myofibroblast markers was increased in SRIF and non-IPF lungs when compared to IPF. Moreover, double immunostaining identified a population of cells expressing both markers (TTF1 and αSMA), which were more frequently stained in SRIF and non-IPF compared to IPF. Furthermore, a significantly higher amount of $TTF1^{+}$ fibroblastic cells were found to reside within the FF of SRIF and non-IPF lungs in comparison to IPF. Our results may indicate that some epithelial cells overlying fibroblastic foci lose the epithelial phenotype and gain the mesenchymal phenotype, contributing at least in part to pulmonary fibrosis. In the present study, we used αSMA and TTF1 as reliable and stable markers for pneumocyte and myofibroblastic differentiation. Our findings are in agreement with Lomas et al. [30], who detected a significant level of αSMA expression in hyperplastic AEC2 in IPF. In addition, Willis et al. [16] analyzed three IPF patients and found that >80% of the lung epithelial cells presented co-expression of TTF1 and αSMA, whereas normal lung tissue contained no cells with both markers. In contrast, Yamada et al. [27] analyzed 15 cases of IPF and were unable to detect cells with dual epithelial/mesenchymal phenotype, even though they made use of various markers (ICAM-1, E-cadherin, CD44v9, LFA, SP-A, and vimentin). However, these markers are not specific to pneumocyte and myofibroblast differentiation. Thus, they could not be used to appropriately address the question raised by these authors. Similar data were described by Morbini et al. [31], who could not support complete EMT, despite the use of several markers (lam5-γ2, fibronectin, vimentin, p63, and E-cadherin). Collectively, these results suggest that some epithelial cells residing in FF lose their epithelial phenotype and gain mesenchymal features. Thus, some fibroblastic cells in FF may originate from epithelial cells.

Mechanistically, our data suggest that EMT is key process contributing to the pathogenesis of pulmonary fibrosis being a possible source of myofibroblasts to FF. However, the EMT may be a reversible process and has been called mesenchymal to epithelial transition (MET). Consequently our findings may not exactly differentiate the way of transition, but show clearly the process. The bone marrow-derived cells may be progenitors of lung alveolar epithelium and has been suggested that EMT/MET might be driven mainly by bone marrow-derived stem cells, which collaborate with local cells to drive chronic, long-term fibrosis. This may be the determining factor for fibrosis severity and could explain discrepancies in the literature related to various subsets of patients (i.e., EMT *vs.* no EMT in IPF) [17,24,28].

One possible explanation that has been raised for the differential findings related to EMT in IPF is the temporal limitation of the EMT phenomenon (i.e., once the cells reach the myxoid stroma they terminally differentiate into myofibroblasts and lose their epithelial characteristics,

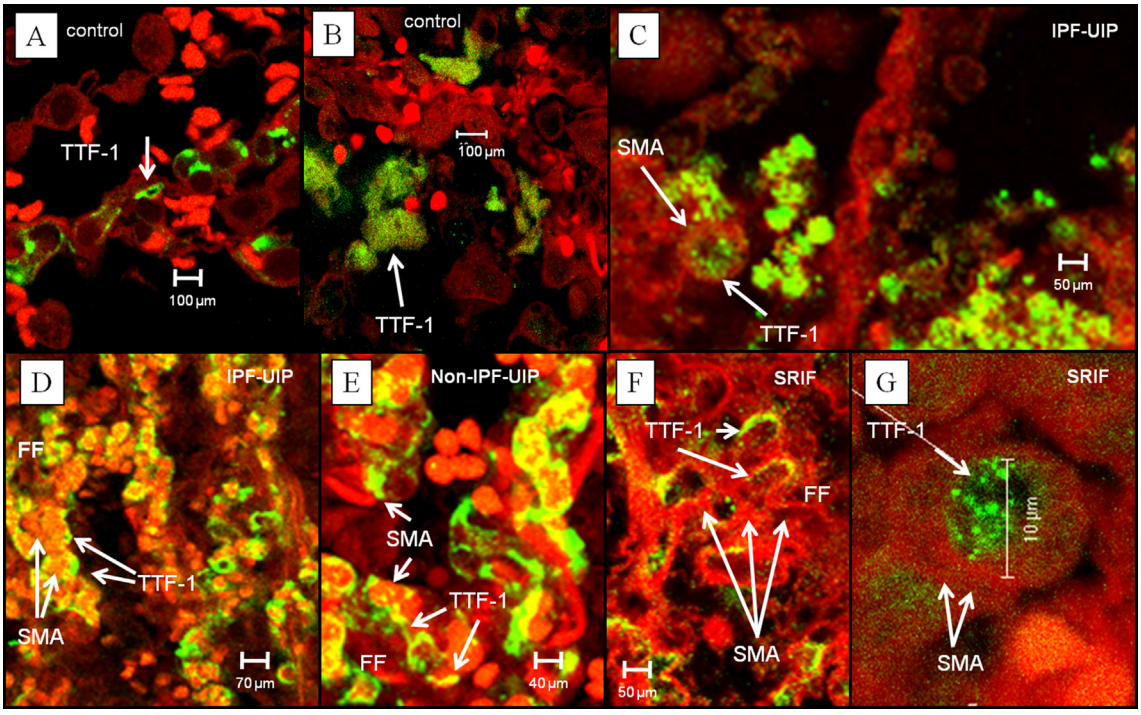

Figure 4 Three-dimensional image reconstruction. Dual immunofluorescence staining reveals TTF1 (green) and αSMA (red) colocalization in FF areas of IPF, non-IPF and SRIF. The nuclear TTF1 immunoreactivity was uniform in pneumocytes of control lungs (arrow) (A); however, the nuclear TTF1 staining of hyperplastic AEC2 led to a diffuse pattern of distribution (B); whereas no αSMA expression was observed in the control groups (A,B). In addition, intense αSMA staining was found in hyperplastic AEC2 (C—G). Hyperplastic AEC2 within FF showed simultaneous staining for epithelial and mesenchymal markers in IPF (C,D), non-IPF (E) and SRIF (F,G). In particular, hyperplastic AEC2 overlying FF showed nuclear TTF1 staining and begin to express cytoplasmtic SMA (G). (For interpretation of the references to color in this figure legend, the reader is referred to the web version of this article.)

including TTF1 expression) as well as the timing of biopsies [27]. Another hypothesis centers on the interaction of the immune system with the EMT process (i.e., potentiation of EMT by inflammatory and/or immune processes). This idea is interesting when considering the higher frequency of lymphocyte aggregates in cases of non-IPF (data not shown). Also, experimental studies indicate greater severity of pulmonary fibrosis in the presence of specific inflammatory responses [32,33]. Additionally, the large number of macrophages in SRIF and the pro-inflammatory activity of cigarette smoke-induced oxidative damage [34] could participate in activating or potentiating EMT by inflammatory mechanisms, potentially worsening the slow course of SRIF and cardiovascular disease-induced UIP.

We hypothesize that precursor cells from the bronchioloalveolar junction move into areas of exposed alveolar septa and initiate regeneration of the epithelial defects. Some of these cells enter the myxoid stroma (EMT), changing their morphology into a spindle shape and upregulating expression of αSMA to enhance their motility. These cells might stimulate the activation of resting fibroblasts/myofibroblasts or even transform fully into myofibroblasts. In addition, it is possible that other stromal cells (resident or bone marrow derived) could access the exposed alveolar surface and undergo MET.

Our results indicate that some epithelial cells within FF lose their epithelial phenotype and gain mesenchymal markers. Thus, we propose that fibroblastic cells within FF originate directly from epithelial cells. Moreover, we observed that this EMT process was more prominent in SRIF and non-IPF compared to IPF; however, the reason for this observation is currently unclear. It is possible that bone marrow-derived cells could be involved in the pathogenesis of IPF. Analysis of TTF1 and αSMA expression represents a reliable and robust method for identifying EMT and MET in lung tissue.

Disclosures of potential conflicts of interest

All authors declare that they have no conflicts of interest.

Financial support

This study was supported by the Coordination for the Improvement of Higher Level Personnel [Capes: 2329-10-7].

References

[1] Katzenstein AL, Myers JL, Prophet WD, Corley 3rd LS, Shin MS. Bronchiolitis obliterans and usual interstitial pneumonia. A comparative clinicopathologic study. Am J Surg Pathol 1986; 10:373—81.

[2] Myers JL, Katzenstein AL. Epithelial necrosis and alveolar collapse in the pathogenesis of usual interstitial pneumonia. Chest 1988;94:1309—11.

[3] Daniil ZD, Gilchrist FC, Nicholson AG, et al. A histologic pattern of nonspecific interstitial pneumonia is associated with a better prognosis than usual interstitial pneumonia in patients with cryptogenic fibrosing alveolitis. Am J Respir Crit Care Med 1999;160:899—905.
[4] Kuhn C, McDonald JA. The roles of the myofibroblast in idiopathic pulmonary fibrosis. Ultrastructural and immunohistochemical features of sites of active extracellular matrix synthesis. Am J Pathol 1991;138:1257—65.
[5] Fukuda Y, Basset F, Ferrans VJ, Yamanaka N. Significance of early intra-alveolar fibrotic lesions and integrin expression in lung biopsy specimens from patients with idiopathic pulmonary fibrosis. Hum Pathol 1995;26:53—61.
[6] Kuhn 3rd C, Boldt J, King Jr TE, Crouch E, Vartio T, McDonald JA. An immunohistochemical study of architectural remodeling and connective tissue synthesis in pulmonary fibrosis. Am Rev Respir Dis 1989;140:1693—703.
[7] King Jr TE, Tooze JA, Schwarz MI, Brown KR, Cherniack RM. Predicting survival in idiopathic pulmonary fibrosis: scoring system and survival model. Am J Respir Crit Care Med 2001; 164:1171—81.
[8] Nicholson AG, Fulford LG, Colby TV, du Bois RM, Hansell DM, Wells AU. The relationship between individual histologic features and disease progression in idiopathic pulmonary fibrosis. Am J Respir Crit Care Med 2002;166:173—7.
[9] American Thoracic S, European Respiratory S. American thoracic Society/European respiratory society international multidisciplinary consensus classification of the idiopathic interstitial pneumonias. This joint statement of the American thoracic society (ATS), and the European respiratory society (ERS) was adopted by the ATS board of directors, June 2001 and by the ERS Executive Committee, June 2001. Am J Respir Crit Care Med 2002;165:277—304.
[10] Visscher DW, Myers JL. Histologic spectrum of idiopathic interstitial pneumonias. Proc Am Thorac Soc 2006;3:322—9.
[11] Katzenstein AL, Mukhopadhyay S, Zanardi C, Dexter E. Clinically occult interstitial fibrosis in smokers: classification and significance of a surprisingly common finding in lobectomy specimens. Hum Pathol 2010;41:316—25.
[12] Kim KK, Kugler MC, Wolters PJ, et al. Alveolar epithelial cell mesenchymal transition develops in vivo during pulmonary fibrosis and is regulated by the extracellular matrix. Proc Natl Acad Sci U S A 2006;103:13180—5.
[13] Wu Z, Yang L, Cai L, et al. Detection of epithelial to mesenchymal transition in airways of a bleomycin induced pulmonary fibrosis model derived from an alpha-smooth muscle actin-Cre transgenic mouse. Respir Res 2007;8:1.
[14] Kasai H, Allen JT, Mason RM, Kamimura T, Zhang Z. TGF-beta1 induces human alveolar epithelial to mesenchymal cell transition (EMT). Respir Res 2005;6:56.
[15] Zhang M, Zhang Z, Pan HY, Wang DX, Deng ZT, Ye XL. TGF-beta1 induces human bronchial epithelial cell-to-mesenchymal transition in vitro. Lung 2009;187:187—94.
[16] Willis BC, Liebler JM, Luby-Phelps K, et al. Induction of epithelial-mesenchymal transition in alveolar epithelial cells by transforming growth factor-beta1: potential role in idiopathic pulmonary fibrosis. Am J Pathol 2005;166:1321—32.
[17] Harada T, Nabeshima K, Hamasaki M, Uesugi N, Watanabe K, Iwasaki H. Epithelial-mesenchymal transition in human lungs with usual interstitial pneumonia: quantitative immunohistochemistry. Pathol Int 2010;60:14—21.
[18] Marmai C, Sutherland RE, Kim KK, et al. Alveolar epithelial cells express mesenchymal proteins in patients with idiopathic pulmonary fibrosis. Am J Physiol Lung Cell Mol Physiol 2011; 301:L71—8.
[19] Nawshad A, Lagamba D, Polad A, Hay ED. Transforming growth factor-beta signaling during epithelial-mesenchymal transformation: implications for embryogenesis and tumor metastasis. Cells Tissues Organs 2005;179:11—23.
[20] Thiery JP. Epithelial-mesenchymal transitions in tumour progression. Nat Rev Cancer 2002;2:442—54.
[21] Liu Y. Epithelial to mesenchymal transition in renal fibrogenesis: pathologic significance, molecular mechanism, and therapeutic intervention. J Am Soc Nephrol JASN 2004;15: 1—12.
[22] Zeisberg M, Yang C, Martino M, et al. Fibroblasts derive from hepatocytes in liver fibrosis via epithelial to mesenchymal transition. J Biol Chem 2007;282:23337—47.
[23] Katzenstein AL, Myers JL. Idiopathic pulmonary fibrosis: clinical relevance of pathologic classification. Am J Respir Crit Care Med 1998;157:1301—15.
[24] Lama VN, Phan SH. The extrapulmonary origin of fibroblasts: stem/progenitor cells and beyond. Proc Am Thorac Soc 2006; 3:373—6.
[25] Kim JH, Jang YS, Eom KS, et al. Transforming growth factor beta1 induces epithelial-to-mesenchymal transition of A549 cells. J Korean Med Sci 2007;22:898—904.
[26] Shintani Y, Maeda M, Chaika N, Johnson KR, Wheelock MJ. Collagen I promotes epithelial-to-mesenchymal transition in lung cancer cells via transforming growth factor-beta signaling. Am J Respir Cell Mol Biol 2008;38:95—104.
[27] Yamada M, Kuwano K, Maeyama T, et al. Dual-immunohistochemistry provides little evidence for epithelial-mesenchymal transition in pulmonary fibrosis. Histochem Cell Biol 2008;129: 453—62.
[28] Pozharskaya V, Torres-Gonzalez E, Rojas M, et al. Twist: a regulator of epithelial-mesenchymal transition in lung fibrosis. PloS One 2009;4:e7559.
[29] Hosper NA, van den Berg PP, de Rond S, et al. Epithelial-to-mesenchymal transition in fibrosis: collagen type I expression is highly upregulated after EMT, but does not contribute to collagen deposition. Exp Cell Res 2013;319:3000—9.
[30] Lomas NJ, Watts KL, Akram KM, Forsyth NR, Spiteri MA. Idiopathic pulmonary fibrosis: immunohistochemical analysis provides fresh insights into lung tissue remodelling with implications for novel prognostic markers. Int J Clin Exp Pathol 2012;5:58—71.
[31] Morbini P, Inghilleri S, Campo I, Oggionni T, Zorzetto M, Luisetti M. Incomplete expression of epithelial-mesenchymal transition markers in idiopathic pulmonary fibrosis. Pathol Res Pract 2011;207:559—67.
[32] Gasse P, Riteau N, Vacher R, et al. IL-1 and IL-23 mediate early IL-17A production in pulmonary inflammation leading to late fibrosis. PloS One 2011;6:e23185.
[33] Mi S, Li Z, Yang HZ, et al. Blocking IL-17A promotes the resolution of pulmonary inflammation and fibrosis via TGF-beta1-dependent and -independent mechanisms. J Immunol 2011; 187:3003—14.
[34] Chilosi M, Poletti V, Rossi A. The pathogenesis of COPD and IPF: distinct horns of the same devil? Respir Res 2012;13:3.